Available online at www.sciencedirect.com
SCIENCE DIRECT®
Journal of Nuclear Materials 347 (2005) 298–306
journal of nuclear materials
www.elsevier.com/locate/jnucmat

Helium and deuterium implantation in tungsten at elevated temperatures

B.B. Cipiti *, G.L. Kulcinski

Fusion Technology Institute, University of Wisconsin, 1500 Engineering Dr., Madison, WI 53706, United States

Abstract

High temperature helium and deuterium implantation on tungsten has been studied using the University of Wisconsin inertial electrostatic confinement device. Helium or deuterium ions from a plasma source were driven into polished tungsten powder metallurgy samples. Deuterium implantation did not damage the surface of the specimens at elevated temperatures (~1200 °C). Helium implantation resulted in a porous surface structure above 700 °C. A helium fluence scan, ion energy scan, and temperature scan were all completed. With 30 keV ions, the pore formation started just below 4×10^{16} He^{+}/cm^{2}. The pore size increased and the pore density decreased with increasing fluence and temperature. The energy scan from 20 to 80 keV showed no consistent trend.
© 2005 Elsevier B.V. All rights reserved.

1. Introduction

The development of any fusion power plant requires a substantial amount of materials engineering research. The reactor chamber wall is subjected to a harsh environment, especially in the case of inertial confinement fusion (ICF) systems. In an ICF design, the first wall receives a repetitive pulse of high-energy particles and X-rays. The material must be able to withstand the heat transients and the effects of the particle flux, all while maintaining structural integrity.

Tungsten is being studied as one of the materials that may be used as armor for the first wall. Tungsten has been a candidate material for fusion walls due to its high melting point and low sputtering yield [1]. However, more research is required on the effects of particle bombardment on the surface of tungsten.

The purpose of this study was to investigate the individual effects of deuterium and helium implantation on tungsten at elevated temperatures. These are two of the ions that will bombard a fusion reactor wall in a deuterium–tritium reactor. The goal was to determine the effects of the implantation on the surface morphology of tungsten, and whether the effects will impact the use of tungsten as armor.

2. Background

The wall of the fusion reactor studied in the high average power laser (HAPL) project will see a variety of fusion ions and reaction products. The helium

* Corresponding author.
E-mail address: bbcipit@sandia.gov (B.B. Cipiti).

0022-3115/$ - see front matter © 2005 Elsevier B.V. All rights reserved.
doi:10.1016/j.jnucmat.2005.08.009

and deuterium ion energies vary from about 1 to 1000 keV [2]. The helium ion spectrum reaches a maximum at about 10^{17} ions/keV (per shot) around the 100–200 keV energy range. The deuterium ion flux reaches a maximum at about 2×10^{18} ions/keV around the 100 keV energy range. It is important to investigate the effects that each of these individual ions have on the wall material.

The average temperature of the first wall surface may be above 600 °C depending on the final design [2]. However, the surface may undergo instantaneous temperatures as high as 2800 °C after the fusion ignition. Therefore, the high temperature effects of the ion implantation are important to determine.

Helium implantation at elevated temperatures has been studied to a limited amount. An experiment done by Thomas and Bauer in 1974 [3] investigated this effect. The implantation of 300 keV helium ions at 2×10^{18} He^{+}/cm^{2} at 1200 °C resulted in the formation of pores on the surface. The authors felt that the pores formed when helium bubbles intersected the surface. They also concluded that the pore formation was stable and resulted in 100% helium reemission upon further helium implantation once it was formed.

Helium is more known for the formation of blisters just below the surface at lower temperature implantation [4]. The blisters form due to helium bubbles forming just below the surface. The problem with blistering is that continued bombardment can cause exfoliation of the chamber surface. Exfoliation should be avoided to increase the wall life of the chamber.

3. Experiment

The University of Wisconsin (UW) inertial electrostatic confinement (IEC) experiment was used for the implantation experiments. The concept works by driving a source of high-energy plasma ions into a metal sample held at a strong negative potential. Fig. 1 shows the experimental setup.

The sample is installed at the end of a high voltage feed through in the center of a vacuum chamber. A boron nitride rod insulates the high voltage conductor. A 50 cm spherical grid made out of stainless steel wires surrounds the sample and is kept at ground potential. A deep potential well forms between the sample and the grid. Three light bulb filaments around the outside of the grid are used to generate ions in a background gas, and control the ion current. Ions that make it past the outer grid are drawn into the sample at the cathode potential.

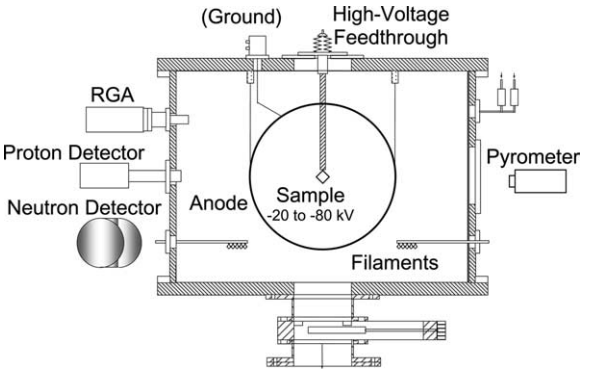

Fig. 1. Ion implantation setup in the UW IEC device.

The chamber is pumped down to background pressures of about 10^{-7} Torr. The implantation gas of interest then flows into the chamber to maintain a constant background pressure of about 0.5 mTorr. This pressure is high enough to maintain the ion flow, yet low enough to prevent collisions that can slow down the ions from the full cathode voltage energy. The power supply of the UW IEC device is capable of 200 kV, 75 mA operation, but the sample roughness limits the maximum voltage due to electrical breakdown problems. The device operates in a steady-state mode.

The tungsten samples were 99.95% tungsten powder metallurgy samples provided by Dr. Lance Snead at Oak Ridge National Laboratory. Both square and round samples were provided, each 1 mm thick. The square samples were 1 cm in length, and the round samples were 1 cm in diameter (see Fig. 2). Each sample was polished on one side, and the average grain size was about 1 μm.

The samples were installed in the chamber as shown in Fig. 3. A tungsten–rhenium wire loop was used to hold the samples in place and connect them to the high voltage line. With this setup, the samples received an ion flux coming in from all angles. The unpolished and polished side both received ion implantation, but only the polished side was used for analysis.

Fig. 4 shows a sample during a typical run. Significant ion power goes into the samples due to the implantation, and the only way to expel the heat is through radiative emission. This allows the IEC setup to be used for high temperature implantation.

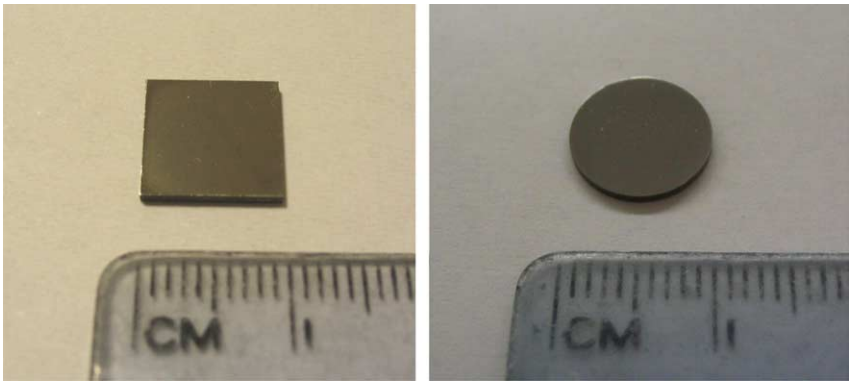

Fig. 2. Tungsten powder metallurgy samples.

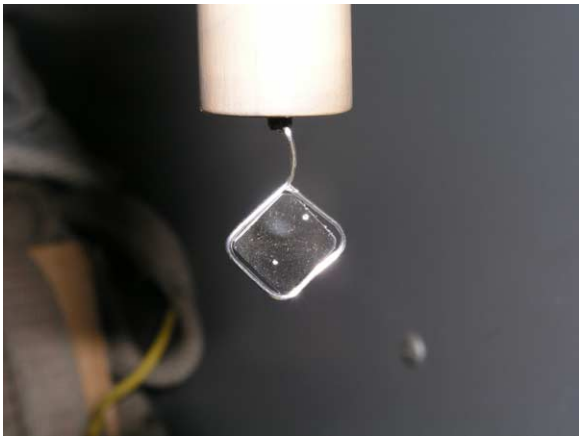

Fig. 3. Tungsten sample installation.

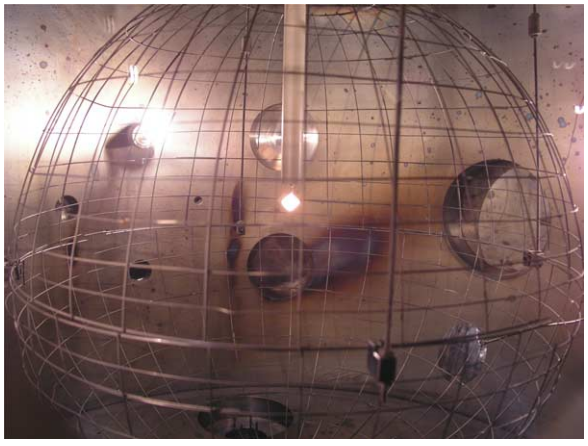

Fig. 4. Tungsten sample during run conditions at 20 kV, 10 mA.

A pyrometer outside of the vacuum chamber is used to measure the temperature of the samples. Because the ion implantation releases secondary electrons, the high voltage power supply meter does not show the true ion current. The pyrometer is a useful tool for determining the actual ion power going into the sample. When a steady-state condition is reached, the power emitted radiatively balances the ion power into the sample. This was used to determine the true ion current, and thus the ion flux reaching the samples.

Fifteen samples were used for the experimentation. For each experiment, a new sample was installed in the chamber for the run, and then it was removed from the chamber for analysis. A scanning electron microscope was used to investigate the effect of the implantation on the surface morphology. Micrographs were taken before and after the implantation. The microscope used was a LEO 1530 field emission scanning electron microscope. It has a resolution of between 1 and 40 nm depending on the voltage. This allowed for very clear pictures of surface features on the order of 0.1 μm. All of the samples were either cleaned or untouched by human hands before scanning. A few standard magnifications were taken of each sample for easy comparison.

Fig. 5 summarizes the experiments that were carried out. One sample was implanted with deuterium up to 2×10^{18} ions/cm^2. The voltage varied between 20 and 40 kV, and the temperature varied between 1100 and 1200 °C. The rest of the experiments were with helium. A helium energy scan was done from 20 to 80 keV at a constant 3×10^{17} He^+/cm^2 fluence and 900 °C temperature. A helium fluence scan was done from 1×10^{16} to 6×10^{17} He^+/cm^2 at a constant 30 keV and with temperature between 800 and 960 °C. Lastly, a helium temperature scan was performed from 700 to 1120 °C at a constant 3×10^{17} He^+/cm^2 fluence and 40 keV.

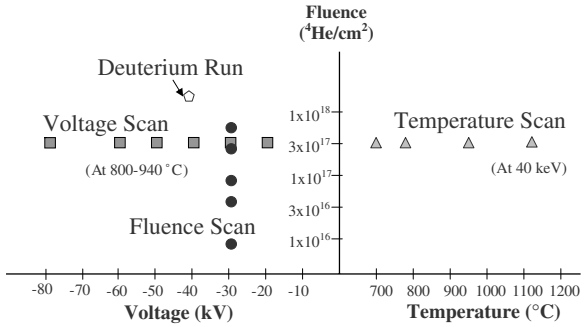

Fig. 5. Tungsten implantation experiments.

4. Results and discussion

The first run using a square sample was with only deuterium. The sample received a total deuterium fluence of 2×10^{18} D^+/cm^2. The voltage was varied between 20 and 40 kV over a total run time of about 32 min. The deuterium implantation did not introduce any observable defects (>0.1 μm) in the surface such as blister or pore formation. Fig. 6 shows a comparison of the sample as received to the sample after the irradiation. The difference is that the irradiated sample experienced significant grain growth. This was most likely just due to the high temperatures reached (1200 °C for about 20 min). The comparison is difficult to make out because the as-received sample was not etched before the experiment, but the as-received grain size was on the order of 1 μm.

The results from the helium implantation were quite a bit different. The helium fluence scan was completed at a constant 30 keV, 6 mA, and 0.5 mTorr helium pressure. The temperature was difficult to control, but the temperature was held between 800 and 960 °C. Fig. 7 shows six micrographs which outline the formation of pores in tungsten at high temperatures.

The upper left tile of Fig. 7 shows the surface of the as-received sample. Sample 2 was implanted with 1×10^{16} He^+/cm^2 at 800 °C. Sample 3 shows the beginning of pore formation at 4×10^{16} He^+/cm^2 at 800 °C. Therefore, the threshold for pore formation is somewhere below the 4×10^{16} He^+/cm^2 level. The pores are localized at the grain boundaries. Sample 4 shows bombardment to 1×10^{17} He^+/cm^2 at 900 °C. The pores have increased in size, and the grain boundaries are no longer discernable. Finally, Samples 5 and 6 show implantation at 3×10^{17} He^+/cm^2 at 920 °C and 6×10^{17} He^+/cm^2 at 960 °C, respectively. It appears that at some point between these two fluences, the pore diameter stabilizes, and the surface structure stabilizes as well.

For each of these micrographs, the average pore diameter and pore density were determined. This was accomplished using the image processing toolbox in MatLab™. The program is able to distinguish the dark areas as pores, and through some manipulation of the picture, it can determine the pore size distribution. The average pore diameter and

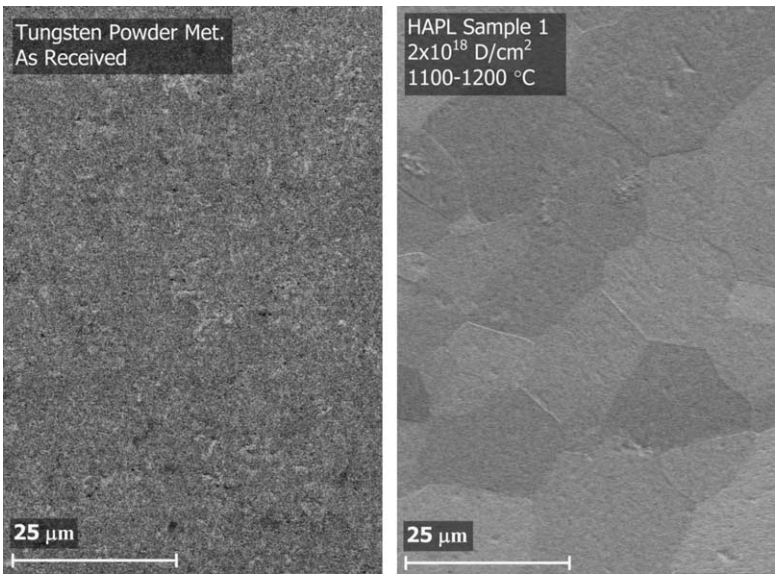

Fig. 6. Deuterium implantation on tungsten showing grain growth.

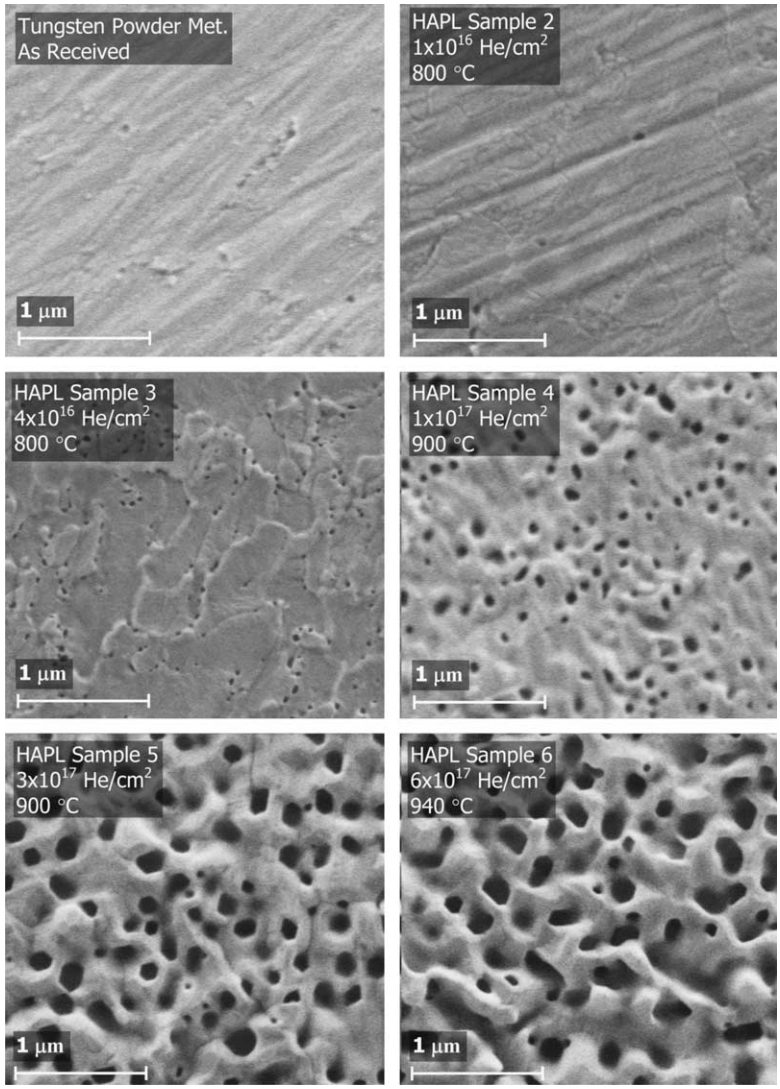

Fig. 7. Fluence scan, $^4He^+$ on tungsten HAPL samples.

density are plotted in Fig. 8. It appears from this plot that the average pore diameter stabilizes around 0.14 μm, and the density stabilizes around 7–8 pores/μm^2.

The next results are for the temperature scan. The energy and fluence were kept constant at 40 keV and 3×10^{17} He^+/cm^2, respectively. Since variation of the current was the only way to control temperature, the flux and time were different for each experiment to still allow for a constant total fluence. If the flux is an important variable in the pore formation, this experiment may not be a good comparison for temperature effects. Fig. 9 shows the results. Sample 7 shows implantation at 700 °C. Visually, the pores are the smallest in this picture. Samples 8 and 9 show slightly larger pores at 770 and 950 °C. Sample 10 has the largest pores at 1120 °C implantation.

The pore diameter and density were plotted for this scan as well (see Fig. 10). This figure does not show a specific type of trend, but over the temperature range from 700 to 1120 °C, the average pore diameter increased by a factor of 6, and the pore density decreased by a factor of 35. If the temperature difference only affects how the helium precipitates, and the total amount is still the same, it makes sense that the 2-D pore density would decrease by about the square of the increase in diameter.

The effects of ion energy did not show a clear trend. In the energy scan, fluence was kept constant

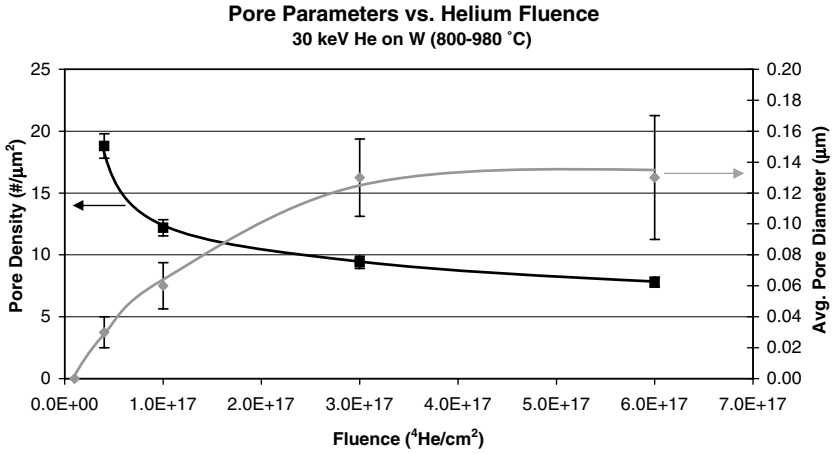

Fig. 8. Increase of pore diameter and decrease of pore density with helium fluence on tungsten.

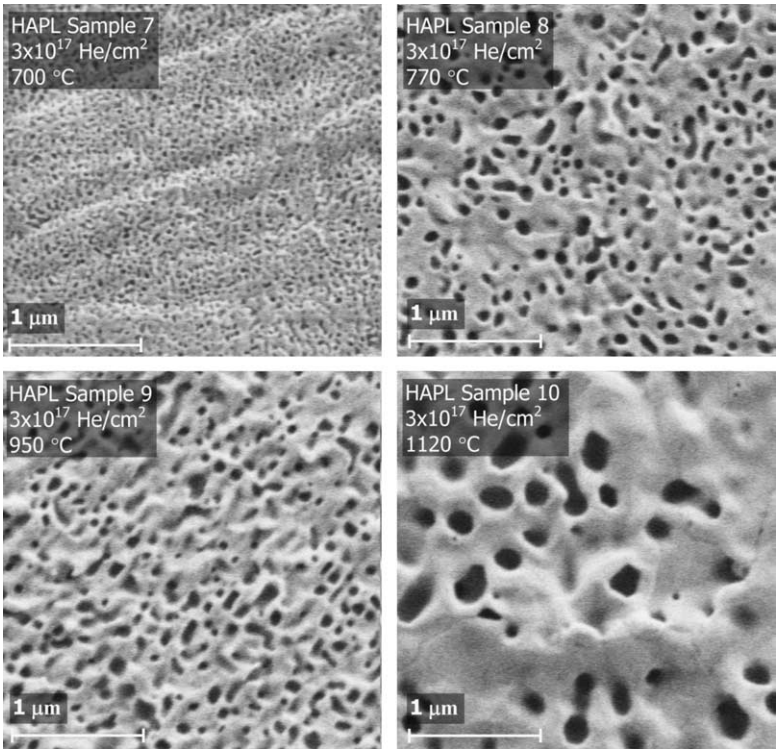

Fig. 9. Temperature scan, $^4He^+$ on tungsten.

at 3×10^{17} He^+/cm^2, and temperature was held between 870 and 940 °C by adjusting the current with the voltage. It is believed that this temperature range is not enough to significantly effect pore size. Fig. 11 shows the results from six samples. It was difficult to control the higher voltages as there were problems with breakdown during the experiments. This led to a variation in the energies. Sample 15 that received 80 keV implantation shows larger pores, and Sample 9 at 40 keV shows slightly smaller pores, but all of the others are about the same. Unfortunately, both the 40 and 80 keV samples were square samples while the others were round. Sample 15 especially was very difficult to control, so it went through a different fluence and energy sequence. The higher voltages experienced electrical

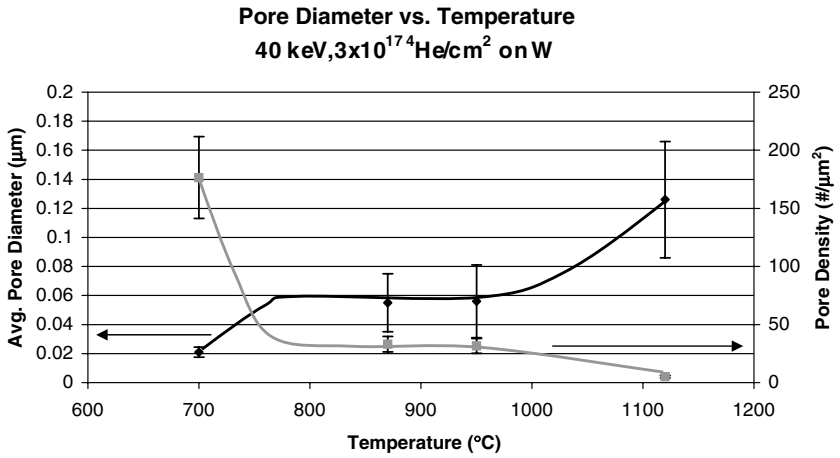

Fig. 10. Increase of pore diameter and decrease of pore density with temperature in tungsten under helium implantation.

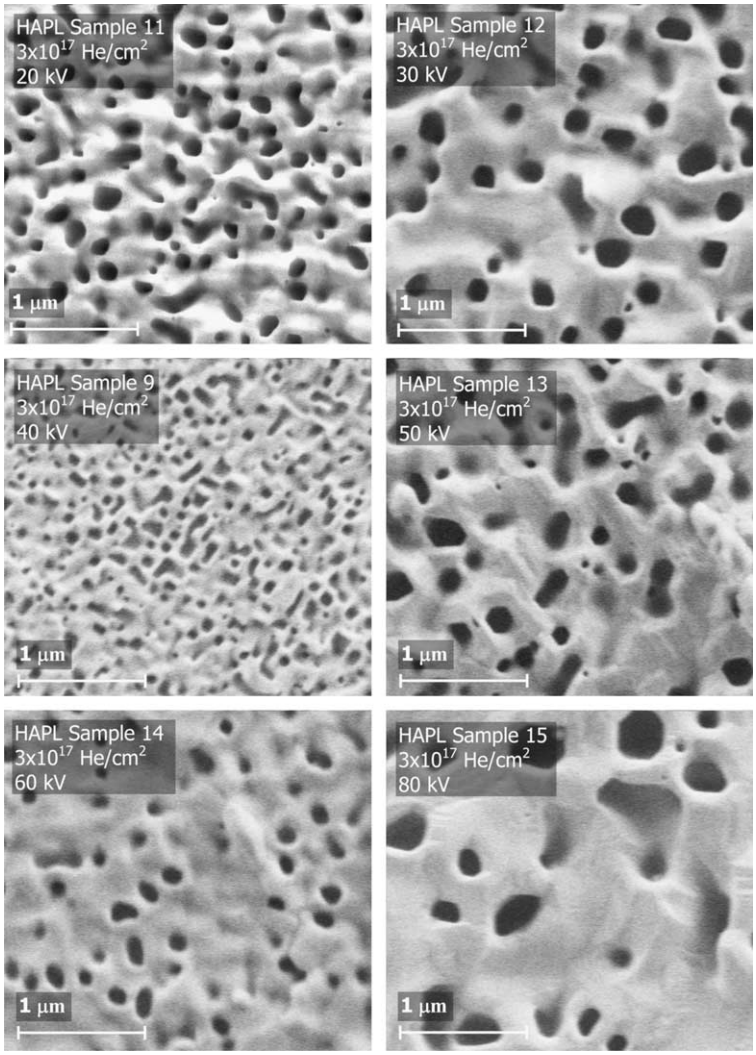

Fig. 11. Voltage scan, $^{4}He^{+}$ on tungsten samples.

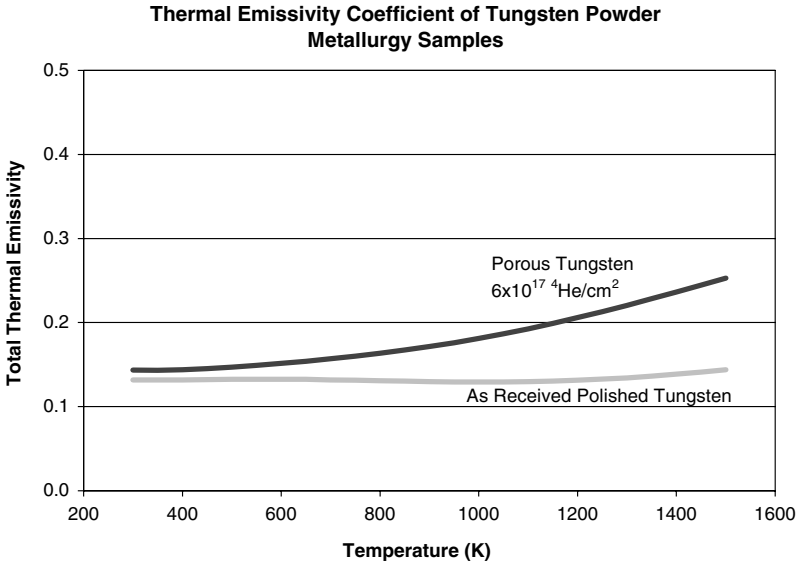

Fig. 12. Change in emissivity with pore formation in tungsten [5].

breakdown problems and current fluctuations. Only the samples at 20, 30, 50, and 60 keV were the same and controlled the best, and they show no clear trend.

As was discussed in Section 2, the true ion current reaching the samples was found by balancing the radiative power out to the input power. In order to do this, the emissivity of the samples was needed. The emissivity was determined by NASA Glenn Research Center with the help of Dr. Don Jaworske and Dr. Duane Beach. Fig. 12 shows the total emissivity as a function of temperature for both the as-received samples and the porous sample that received the highest helium fluence (6×10^{17} He^+/cm^2). These values were used in all of the calculations.

5. Conclusions

The deuterium implantation did not show any deformation in tungsten at high temperatures. At the higher temperatures, the deuterium probably diffuses out of the tungsten rapidly to prevent the buildup of gases. It would be useful to determine the effects of both deuterium and helium implantation at the same time to determine if the deuterium can get trapped in helium bubbles.

The porous surface structure due to helium implantation developed at a relatively low fluence. The largest helium fluence reached in these experiments, 6×10^{17} He^+/cm^2, will be reached by the reference HAPL chamber after 8 h of operation [6]. This calculation includes the total helium fluence expected over the entire energy range.

The porous structure probably occurs as helium bubbles migrate to the surface. The erosion of the tungsten was not measured in this experimentation, but would be useful to know in the future. It appears that the pore formation prevents the exfoliation that can accompany blistering. Therefore, it may mean that tungsten will last longer in the HAPL chamber if it is maintained at a higher temperature.

Future experiments should compare erosion rates in tungsten when blistering occurs (at room temperature) to the erosion rates in tungsten when pores are formed (at elevated temperatures). In addition, this experiment only focused on a small range of the helium energies expected on the HAPL chamber wall. Further experimentation must be done at the full range of energies to investigate if this porous structure still forms even with deeper implantation depths.

Acknowledgements

This work was partially supported by the Naval Research Laboratory. The research was performed under appointment to the Fusion Energy Sciences Fellowship Program administered by Oak Ridge Institute for Science and Education under a contract between the US Department of Energy and Oak Ridge Associated Universities.

The samples for these experiments were provided by Dr Lance Snead and Dr Steve Zinkle at Oak Ridge National Laboratory. The true ion current calculations were made much easier with emissivity measurements done by Dr Don Jaworske and Dr Duane Beach at NASA Glenn Research Center. Finally, the authors would like to thank the other members of the Wisconsin IEC project: Bob Ashley, John Santarius, Greg Piefer, S. Krupakar Murali, Ross Radel, Alex Wehmeyer, Dave Boris, and Tracy Uchytil.

References

[1] G. Federici et al., Nucl. Fusion 41 (2001) 1967.
[2] J.D. Sethian et al., Nucl. Fusion 43 (2003) 1693.
[3] G.L. Thomas, W. Bauer, J. Nucl. Mater. 53 (1974) 134.
[4] M. Kaminsky, Radiation Effects on Solid Surfaces, American Chemical Society, Washington, D.C., 1976.
[5] D. Jaworske, D. Beach, NASA Glenn Research Center, 2004, unpublished results.
[6] R.R. Peterson, Los Alamos National Laboratory, Private communication, 2003.